International Journal of Architectural, Civil and Construction Sciences
ISSN: 2415-1734
Vol:14, No:11, 2020

Seismic Fragility Assessment of Strongback Steel Braced Frames Subjected to Near-Field Earthquakes

Mohammadreza Salek Faramarzi, Touraj Taghikhany

***Abstract*—**In this paper, seismic fragility assessment of a recently developed hybrid structural system, known as the strongback system (SBS) is investigated. In this system, to mitigate the occurrence of the soft-story mechanism and improve the distribution of story drifts over the height of the structure, an elastic vertical truss is formed. The strengthened members of the braced span are designed to remain substantially elastic during levels of excitation where soft-story mechanisms are likely to occur and impose a nearly uniform story drift distribution. Due to the distinctive characteristics of near-field ground motions, it seems to be necessary to study the effect of these records on seismic performance of the SBS. To this end, a set of 56 near-field ground motion records suggested by FEMA P695 methodology is used. For fragility assessment, nonlinear dynamic analyses are carried out in OpenSEES based on the recommended procedure in HAZUS technical manual. Four damage states including slight, moderate, extensive, and complete damage (collapse) are considered. To evaluate each damage state, inter-story drift ratio and floor acceleration are implemented as engineering demand parameters. Further, to extend the evaluation of the collapse state of the system, a different collapse criterion suggested in FEMA P695 is applied. It is concluded that SBS can significantly increase the collapse capacity and consequently decrease the collapse risk of the structure during its life time. Comparing the observing mean annual frequency (MAF) of exceedance of each damage state against the allowable values presented in performance-based design methods, it is found that using the elastic vertical truss, improves the structural response effectively.

***Keywords*—**Strongback System, Near-fault, Seismic fragility, Uncertainty, IDA, Probabilistic performance assessment.

I. Introduction

ONE of the cost-effective structural systems which are used frequently by engineers is the concentrically braced frame (CBF) because of their advantages such as significant lateral stiffness and proper energy dissipation. However, the occurrence of the soft-story mechanism and the concentration of demands in specific stories have been among the important challenges that researchers deal with in past decades. The abrupt change in lateral stiffness as a result of compression brace buckling in adjacent stories results in damage concentration and large residual drift ratio. Hence, many researchers proposed various solutions to mitigate the soft-story mechanism and decline the residual drift ratio of stories [1]. In this regard, Mahin and Lai [1] suggested a new hybrid bracing system called the SBS, which is a retrofit of CBFs and stems from zipper braced frames, tied eccentrically braced frames, and an elastic truss system. In this system, the braced span consists of two different segments; I) an elastic vertical truss namely the strongback spine, which imposes a nearly uniform distribution of story displacement over the height of the building, and II) an inelastic braced frame for energy dissipation. The strongback spine is designed to remain essentially elastic during earthquake excitation which consequently keeps the structure from damage concentration and results in lower residual drift ratio [1], [2]. In Fig. 1, the effect of the strongback spine on distribution of story displacement and prevention of soft-story mechanism is illustrated.

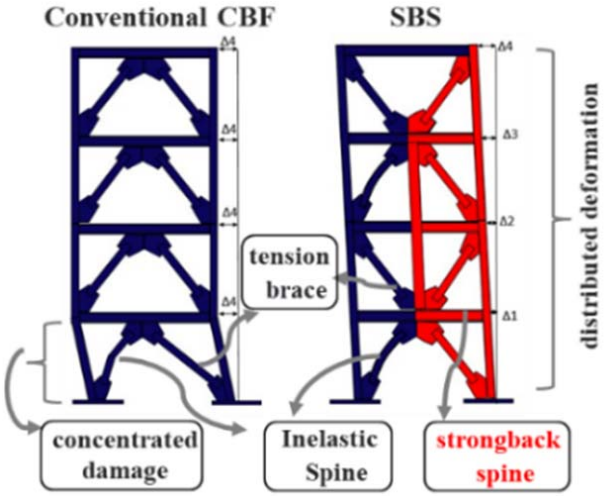

Fig. 1 The effect of strongback spine on distribution of displacement throughout the structure

The strongback spine is designed as a vertical steel truss (elastic conventional CBFs) or rigid steel plate shear wall that responds elastically during the ground excitation. Some SBS configurations are depicted in Fig. 2 using conventional steel braces or steel plate shear walls as strongback spine. On the other hand, because of distinctive characteristics of near-fault excitations such as high-velocity pulses, they can generate large engineering demands in structure. These effects have not been investigated comprehensively in strongback braced frames yet. Hence, this study is focused on the effect of these ground motion records on the structural response of the SBS. To this end, the seismic fragility assessment of the SBS is carried out according to HAZUS multi-hazard loss estimation

Mohammadreza Salek Faramarzi is with the Department of Civil and Environmental Engineering, Amirkabir University of Technology, Tehran, Iran (corresponding author, phone: (+98) 26 3421 2983; e-mail: mreza.salekfar@ gmail.com).
Touraj Taghikhany is with the Department of Civil and Environmental Engineering, Amirkabir University of Technology, Tehran, Iran (e-mail: ttaghikhany@aut.ac.ir).

methodology [3] and FEMA P695 guideline [4].

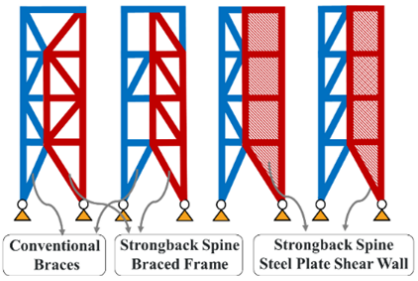

Fig. 2 Different SBS configurations

II. Performance-Based Earthquake Engineering (PBEE)

In PBEE provisions, to evaluate the performance objectives of structures, engineering demand parameters (EDP) are compared against the damage measures (DM) corresponding to the intensity measure (IM) for each earthquake record. For each IM value of x, if the probability of EDP exceeds a y value, it can be presented as $G(EDP \geq y|IM = x)$ [5]. In this study, to evaluate the seismic fragility of SBS, the recommended provision presented in HAZUS program technical manual [3] is used. To this end, four different damage states including slight (DS1), moderate (DS2), extensive (DS2), and complete structural damage (DS3) are considered according to [3]. Maximum inter-story drift ratio (MIDR) and peak floor acceleration (PFA) are selected as EDPs for structural and non-structural damages, respectively. The recommended DM values for each considered damage state are shown in Table I. These values corresponded to high-rise steel braced buildings (eight-story and up) and high-code seismic design level. Following to HAZUS methodology [3], it is supposed that dominant parameters for seismic fragility assessment of structures are independent so that each seismic fragility curve is extracted based on a particular failure threshold. Further, to extend the outcomes of the seismic fragility assessment of the SBS, the FEMA P695 [4] methodology is used to investigate the collapse probability of the system subjected to the considered near-field ground motion records.

TABLE I
Recommended DM Values for Considered Damage States According to HAZUS [3]

Damage State	Slight	Moderate	Extensive	Complete
MIDR	0.0031	0.0063	0.0188	0.0500
PFA	0.45 g	0.9 g	1.8 g	3.6 g

III. Ground Motion Records

Due to some significant characteristics of near-field ground motions, the structural responses have distinguished differences in comparison to those experienced in far-field records. Although there is no general description for the near-fault zone to consider if a site may be classified as near or far-field, the near-fault zone is typically considered to be within a distance of about 30 km from the fault rupture [5], [6]. In this paper, a set of 28 near-field records (56 single horizontal components) is used which are suggested by FEMA P695 [4]. The set of applied near-field records consists of 14 pulse-like records and fourteen non-pulse-like records using wavelet analysis method proposed by Baker [7]. The records characteristics such as soil type, PGA, PGV, magnitude, and epicentral distance are listed in the Appendix.

IV. Seismic Design of the Building

Here, an eight-story strongback steel-braced structure is considered to assess the seismic fragility response of the system under specified near-field ground motion records. It is assumed that the building is located in Van Nuys, California, and has the geometries shown in Fig. 3. As shown in this figure, each direction has five bays, and the bay widths are equal to 6.1 m. All beam-to-column connections except those in the braced bay are of hinge type. Thus, two perimeter lateral load-resisting frames, each composed of two braced bays, bear seismic loads in each direction.

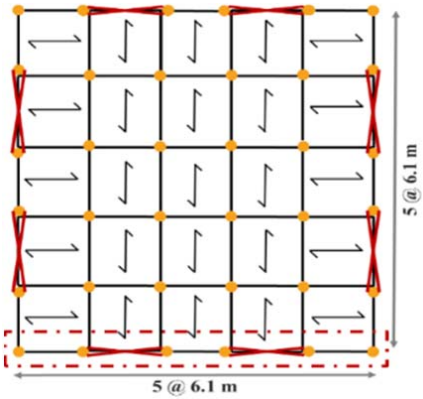

(a) Plan view of a typical story

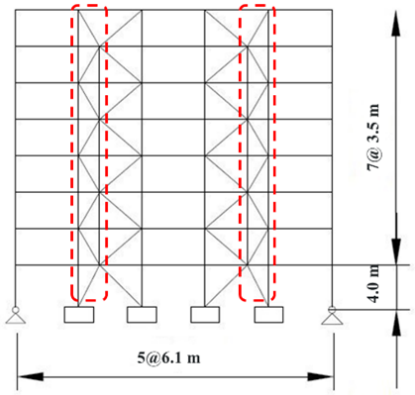

(b) Elevation of the building

Fig. 3 SBS design properties

For building design, prescriptive specifications of ASCE7-16 [8] and AISC360-16 [9] standards are followed using the direct analysis method, with stiffness reduction (based on the $0.8\tau_b$ method) applied to all members. Regarding the assumed building's location (Van Nuys, California), D soil type, and

spectral acceleration coefficients $S_{D1} = 0.778$ and $S_{DS} = 1.4887$. The design earthquake base shear is computed by considering the importance factor $I = 1.0$ and seismic design category $SDC = D$. Gravity loading of the buildings includes dead and live uniform loads equal, respectively, to 5 and 2.5 KN/m^2 along with perimeter wall loads that equal 8.5 and 2.7 KN/m in roof and stories, respectively. The section properties of designed members are presented in Fig. 3. For designing the SBS, to create an elastic vertical truss, the strongback members are selected so that the stress ratio in all of them is lower than 0.5, which is the inverse of the over-strength factor chosen for this system, requires the stress ratios equal to it to achieve elastic and non-yielding behavior.

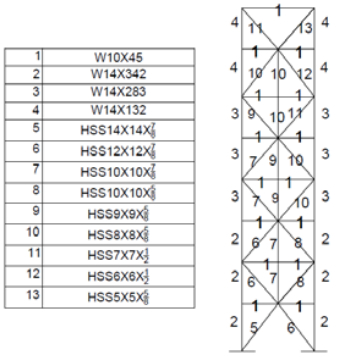

Fig. 4 Detail member sections of the SBS

V. Numerical Modeling

The numerical modeling method utilized in this article, is based on recent results of valid experiments on steel braced frames including [10], [1], and [2]. In this study, the building shown in Fig. 2 is modeled in two dimensions using OpenSees [11] software. For this purpose, the plan symmetry is used and the buildings behavior in X direction is represented by a single braced frame. The effect of interior columns on amplifying the p-delta forces in the modeled frame is simulated using leaning columns. The numerical modeling details are presented in Fig. 4. As shown in this figure, force-formulated fiber elements are used for modeling the structural members using uniaxial steel02 material in OpenSees [11] with 0.003 kinematic strain hardening. A 2% critical damping value was considered for the structure.

To account for the loss of strength and stiffness due to local buckling of the brace section during loading cycles, a low-cycle fatigue model is attributed to the stress-strain behavior of the brace material according to [10]. To validate the proficiency of the numerical modeling method applied in this study, the lateral force-displacement hysteresis curves of the model in this study have been compared against the experimental results presented by [10] in Fig. 6. The figure shows well agreement between the obtained results from the model in this study with experimental test and numerical outcomes.

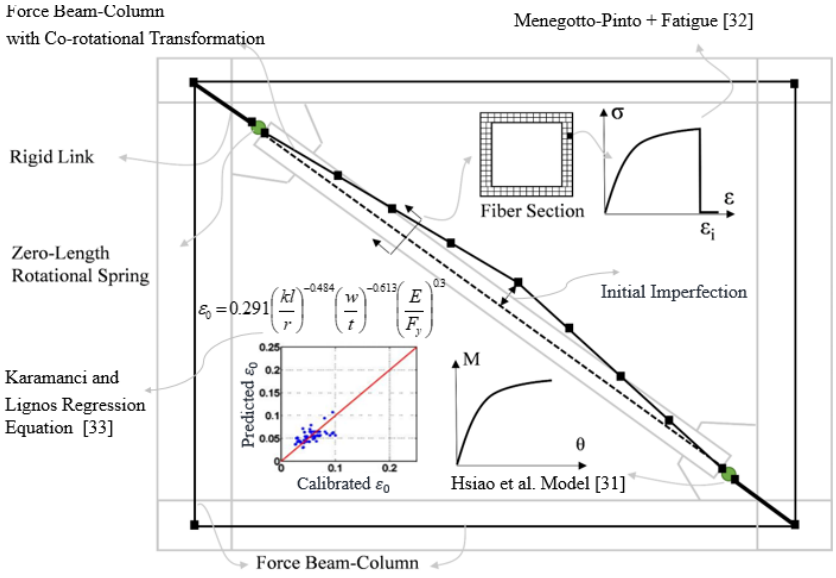

Fig. 5 Nonlinear modeling details used in this study

VI. Incremental Dynamic Analysis

Incremental dynamic analysis (IDA) is performed based on the hunt & fill algorithm proposed by [12]. Using an appropriate IM is of significant importance for a precise evaluation of structural response. Therefore, in this paper first mode spectral acceleration Sa(T1) is used as IM according to FEMA P695 [4] methodology. As stated before, MIDR (θ_{MIDR}) and PFA (θ_{roof}) are selected as EDP to evaluate the structural performance. The resulting IDA curves of the SBS are illustrated in Fig. 6 using θ_{MIDR} and θ_{roof} as EDP.

The MAF of each fragility can be next calculated by integrating the fragility function over the hazard curve of the building's location (Fig. 7). According to defined damage states presented in Table II, fragility curves of each damage

state considering MIDR and PFA as EDPs are derived using cumulative distribution function and presented in Fig. 8.

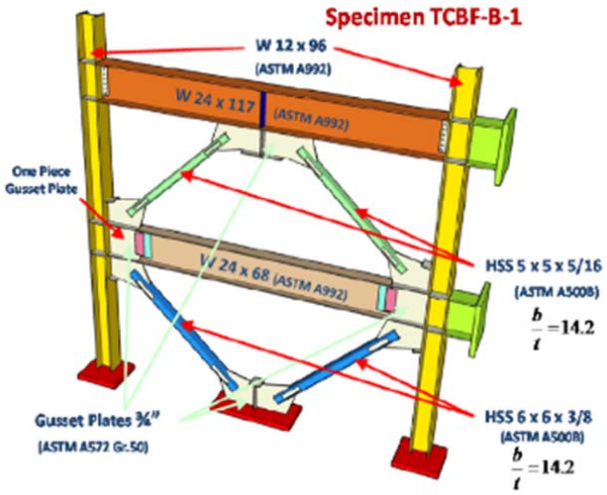

(a) TCBF-B-1 specimen configuration [14]

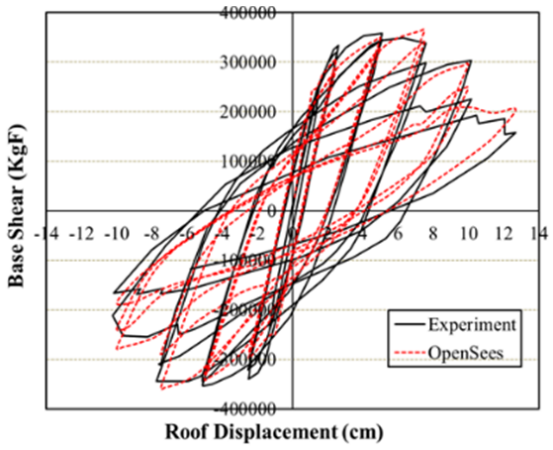

(b) Numerical vs. experimental hysteresis curves

Fig. 6 Nonlinear modeling method verification

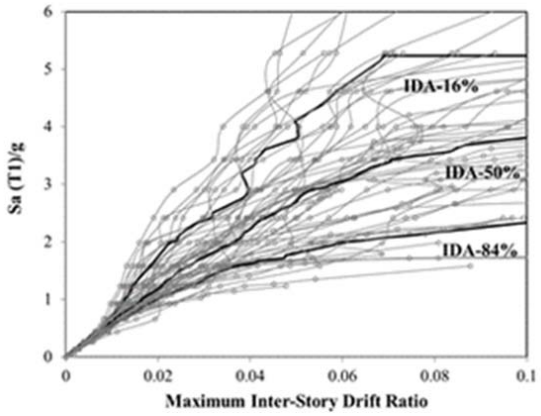

(a) MIDR

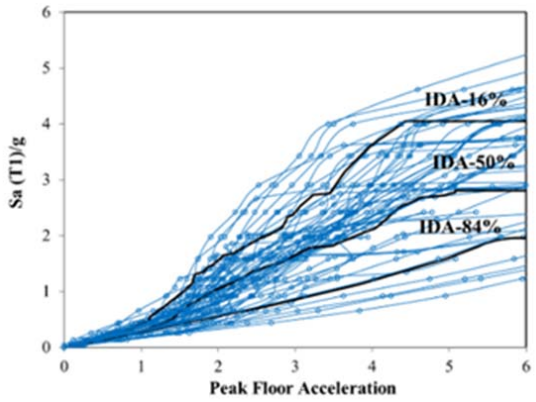

(b) Peak roof drift ratio

Fig. 7 IDA results

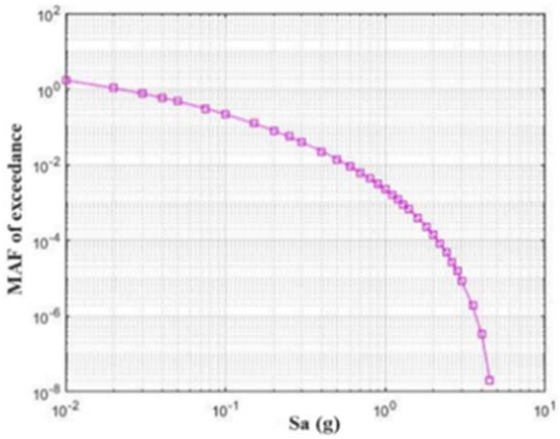

Fig. 8 Seismic hazard curve for the site

VII. Probabilistic Performance Assessment

To compute the MAF of each fragility, (1) which is a closed-formed equation proposed by [13] to simplify the implementation of the procedure is used:

$$\lambda_{LS} = H(\hat{s}_{LS}).\exp(0.5k^2\beta_{T\theta}^2) \quad (1)$$

where λ_{LS} denotes MAF of exceeding limit state fragility, $\hat{s}_{LS}$ denotes the median S_a value of the LS fragility, and $H(\hat{s}_{LS})$ is its exceedance MAF according to the relevant seismic hazard curve. The k parameter denotes the tangent slope of the hazard curve at $\hat{s}_{LS}$ and, $\beta_{T\theta}$ is the dispersion of the LS fragility function. For computing the hazard slope k, [14] proposed (2) for calculating the slope of the hazard secant line passing through the two s_1 and s_2 intensity values. The s_1 and s_2 values are proposed to be computed at the vicinity of $\hat{s}_{LS}$ and by considering the dispersion of LS fragility using (3):

$$K = \frac{\ln H(s_2) - \ln H(s_1)}{\ln(s_2) - \ln(s_1)} \quad (2)$$

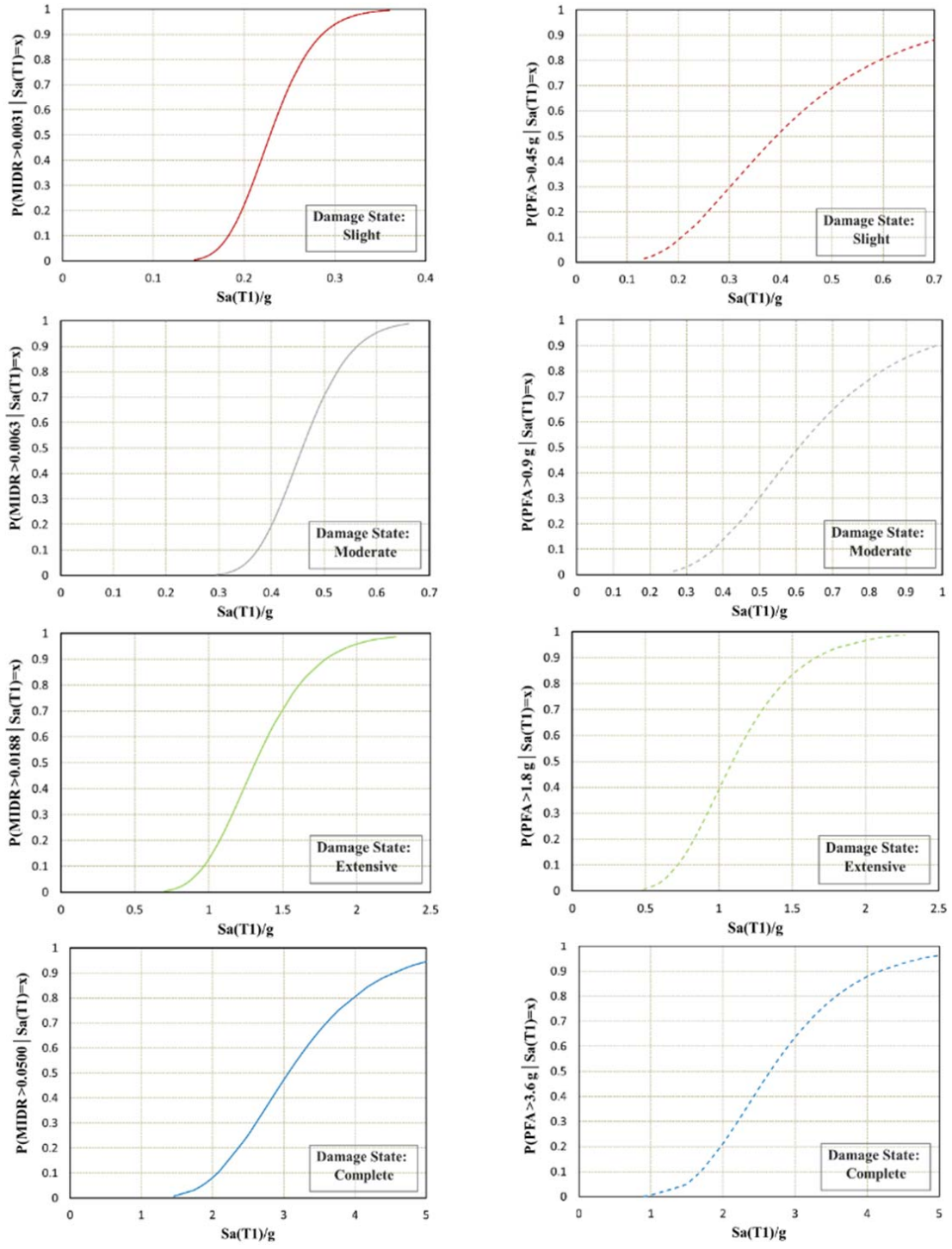

(a) MIDR-based (b) PFA-based

Fig. 9 Seismic fragility curves of the structure for different damage states

$$\left\{\begin{matrix} s_1 = \hat{s}_{LS}.\exp(-0.5\beta_{T\theta}) \\ s_2 = \hat{s}_{LS}.\exp(-1.5\beta_{T\theta}) \end{matrix}\right\} \quad (3)$$

To determine the associated total uncertainty value for each damage state, appropriate epistemic uncertainty (β_{USc}) and aleatory uncertainty (β_{Sc}) values should be selected. Here, according to [15], a 0.2 epistemic uncertainty value is considered for DS1 and DS2, and a value of 0.3 for DS3 and

DS4. It should be noted that different parameters affect the selection of proper uncertainty value including nonlinear modeling method, nonlinear method, seismic response threshold, etc. Also, for the aleatory uncertainty, the proposed equation by [16], (4), is applied using IDA results.

$$\beta_{T\theta}=\sqrt{\beta_{USc}^2+\beta_{Sc}^2} \qquad ,\beta_{Sc}=0.5\times\left(\ln S_{aC}^{84\%}-\ln S_{aC}^{16\%}\right) \tag{4}$$

where $S_{ac}^{16\%}$ and $S_{ac}^{84\%}$ are 16% and 84% fractiles of $S_a(T1)$–capacity. The selected uncertainty values for each damage state are presented in Table III. Having these values, the probability of exceeding each fragility limit state in 50 years can be determined using the Poisson distribution function according to (5):

$$P(\lambda,t)=1-\exp(-\lambda t) \tag{5}$$

where t is the time (years). The summary of results is shown in Table III. Comparing the observed MAF values of the structure against the allowable exceedance probability of equal damage states in performance-based design guidelines such FEMA 356 [17], the MAF of exceedance of each damage state is nearly less than or equal to the accepted ones. So it can be concluded that using the proposed design strategy, the SBS met the desired performance targets.

TABLE II
SUMMARY RESULTS OF THE OBSERVED MAF OF EACH DAMAGE STATE AND THE PROBABILITY OF OCCURRENCE

	Damage State							
	Slight		Moderate		Extensive		Complete	
	$MIDR$ $= 0.0031$	PFA $= 0.45$ g	$MIDR$ $= 0.0063$	$PFA = 0.9$g	$MIDR$ $= 0.0188$	$PFA = 1.8$ g	$MIDR$ $= 0.050$	PFA $= 3.6$ g
$S_{ac}^{16\%}$	0.176	0.737	0.397	1.447	0.968	2.256	1.850	4.124
$S_{ac}^{50\%}$	0.220	0.834	0.440	1.558	1.144	2.705	2.728	5.327
$S_{ac}^{84\%}$	0.228	0.843	0.446	1.680	1.628	3.161	3.828	6.151
(β_{Sc})	0.13	0.07	0.05	0.07	0.26	0.17	0.36	0.21
$(\beta_{T\theta})$	0.24	0.30	0.21	0.22	0.39	0.34	0.47	0.36
MAF (λ)	0.0557	0.1016	0.0149	0.0465	0.00148	0.02127	0.00045	0.00037
Probability	0.93	0.99	0.52	0.90	0.07	0.65	0.02	0.01

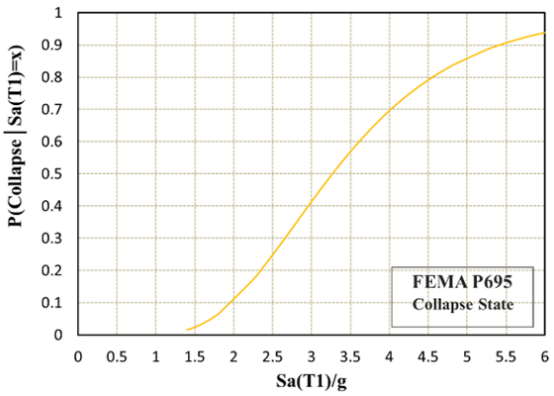

Fig. 10 Collapse fragility curve according to FEMA P695 [4]

TABLE III
SBS COLLAPSE PERFORMANCE ASSESSMENT RESULTS

$\hat{S}_{CT}$ (g)	CMR	$\lambda_{Collapse}$	Collapse Probability
3.28	2.19	0.00004	0.0019

VIII. CONCLUSION

In this study, to investigate the seismic fragility curves of a hybrid steel bracing system, called the SBS, a set of 56 near-field ground motion records presented in FEMA P695 were used including pulse-like and non-pulse-like records. For performance assessment purposes, the recommended framework in HAZUS guideline was implemented. Also, the collapse fragility curve of the SBS was studied in accordance with FEMA P695 methodology. Different sources of uncertainty were taken to account to have a proper structural performance evaluation. Based on IDA results, it is found that the MAF of exceedance of each damage state is almost less than or equal to the accepted ones that are suggested by performance-based design guidelines. The median collapse capacity and the collapse margin ration (CMR) of the SBS were 3.28 g and 2.19, respectively. The exceedance probability of slight damage state (DS1) for both MIDR and PFA was more than 90%. According to the results, it can be concluded that using the proposed design strategy for strongback spine, the SBS would meet the desired performance targets appropriately.

APPENDIX

TABLE IV
INFORMATION OF SELECTED GROUND MOTIONS

No.	Record	Station	Soil Type	MAX. PGA (g)	MAX. PGV (cm/s)	Mw	Epicentral (km)
Pulse Records Subset							
1	Imperial Valley-06	El Centro Array #6	D	0.44	111.9	6.5	27.5
2	Imperial Valley-06	El Centro Array #7	D	0.46	108.9	6.5	27.6
3	Irpinia, Italy-01	Sturno	B	0.31	45.5	6.9	30.4
4	Superstition Hills-02	Parachute Test Site	D	0.42	106.8	6.5	16.0
5	Loma Prieta	Saratoga - Aloha	C	0.38	55.6	6.9	27.2
6	Erzican, Turkey	Erzincan	D	0.49	95.5	6.7	9.0
7	Cape Mendocino	Petrolia	C	0.63	82.1	7.0	4.5
8	Landers	Lucerne	C	0.79	140.3	7.3	44.0
9	Northridge-01	Rinaldi Receiving Sta	D	0.87	167.3	6.7	10.9
10	Northridge-01	Sylmar - Olive View	C	0.73	122.8	6.7	16.8
11	Kocaeli, Turkey	Izmit	B	0.22	29.8	7.5	5.3
12	Chi-Chi, Taiwan	TCU065	D	0.82	127.7	7.6	26.7
13	Chi-Chi, Taiwan	TCU102	C	0.29	106.6	7.6	45.6
14	Duzce, Turkey	Duzce	D	0.52	79.3	7.1	1.6
No Pulse Records Subset							
15	Gazli, USSR	Karakyr	C	0.71	71.2	6.8	12.8
16	Imperial Valley-06	Bonds Corner	D	0.76	44.3	6.5	6.2
17	Imperial Valley-06	Chihuahua	D	0.28	30.5	6.5	18.9
18	Nahanni, Canada	Site 1	C	1.18	43.9	6.8	6.8
19	Nahanni, Canada	Site 2	C	0.45	34.7	6.8	6.5
20	Loma Prieta	BRAN	C	0.64	55.9	6.9	9.0
21	Loma Prieta	Corralitos	C	0.51	45.5	6.9	7.2
22	Cape Mendocino	Cape Mendocino	C	1.43	119.5	7.0	10.4
23	Northridge-01	LA - Sepulveda VA	C	0.73	70.1	6.7	8.5
24	Northridge-01	Northridge - Saticoy	D	0.42	53.2	6.7	3.4
25	Kocaeli, Turkey	Yarimca	D	0.31	73.0	7.5	19.3
26	Chi-Chi, Taiwan	TCU067	C	0.56	91.8	7.6	28.7
27	Chi-Chi, Taiwan	TCU084	C	1.16	115.1	7.6	8.9
28	Denali, Alaska	TAPS Pump Sta. #10	C	0.33	126.4	7.9	7.0

REFERENCES

[1] Lai, J.W. and Mahin, S.A.; "Strongback system: A way to reduce damage concentration in steel-braced frames", Journal of Structural Engineering, 141(9): 04014223, 2015.
[2] Simpson, B.G. and Mahin, S.A.; "Experimental and numerical investigation of strongback braced frame system to mitigate weak story behaviour", Journal of Structural Engineering, 144(2): 04017211, 2018.
[3] FEMA-NIBS; "Earthquake Loss Estimation Methodology, HAZUS-MH MR4, Technical Manual", Federal Emergency Management Agency and National Institute of Building Sciences: Washington, U.S.A., 2003.
[4] FEMA P695; "Quantification of Building Seismic Performance Factors", Federal Emergency Management Agency, Washington, U.S.A., 2009.
[5] Bozorgnia Y. and Bertero, V.V.; "Earthquake Engineering: form Engineering Seismology to Performance-Based Engineering", CRC Press, U.S.A., 2004.
[6] Alavi, B. and Krawinkler, H.; "Behavior of moment-resisting frame structures subjected to near-fault ground motions", Earthquake engineering and structural dynamics, 33(6): 687-706, 2004.
[7] Baker, J.W.; "Quantitative classification of near-fault ground motions using wavelet analysis", Bulletin of the Seismological Society of America, 97(5):1486-1501, 2007.
[8] ASCE/SEI 7-16; "Minimum design loads and associated criteria for buildings and other structures", American Society of Civil Engineers, Reston, Virginia, U.S.A., 2017.
[9] AISC 360-16, "Specification for Structural Steel Buildings", American Institute of Steel Construction, U.S.A., 2016.
[10] Uriz, P. and Mahin, S. A.; "Toward Earthquake-Resistant Design of Concentrically Braced Steel-Frame Structures", Pacific Earthquake Engineering Research Center, University of California, Berkeley, C. A., U.S.A., 2008.
[11] Mazzoni, S., McKenna, F., Scott, M.H. and Fenves, G.L.; "OpenSees user's manual", Pacific Earthquake Engineering Research Center, University of California, Berkeley, C. A., U.S.A., 18: 56-57, 2004.
[12] Vamvatsikos, D. and Cornell, C. A.; "Incremental Dynamic Analysis", Earthquake Engineering and Structural Dynamics, 31(3): 491–514, 2002.
[13] Cornell, C. A., Jalayer, F., Hamburger, R. O. and Foutch, D. A.; "The Probabilistic Basis for the 2000 SAC/FEMA Steel Moment Frame Guidelines", Journal of Structural Engineering, 128(4): 526-533, 2002.
[14] Vamvatsikos, D.; "Accurate Application and Second-Order Improvement of the SAC/FEMA Probabilistic Formats for Seismic Performance Assessment", Journal of Structural Engineering, 140(2): 04013058, 2014.
[15] Vamvatsikos, D. and Aschheim, M.; "Yield Frequency Spectra and Seismic Design of Code-Compatible RC Structures: An Illustrative Example", Earthquake Engineering and Structural Dynamics, 35(11): 1759-1778, 2016.
[16] Vamvatsikos, D. and Fragiadakis, M.; "Incremental Dynamic Analysis for Estimating Seismic Performance Sensitivity and Uncertainty", Earthquake Spectra, 39: 141–163, 2010.
[17] FEMA 356; "Prestandard and Commentary for the Seismic Rehabilitation of Buildings", Federal Emergency Management Agency, Washington, U.S.A., 2000.